nature communications

Article

https://doi.org/10.1038/s41467-026-75288-y

Identification of carnivory in the flowering plant *Saxifraga* via multidisciplinary evidence

Received: 5 September 2025

Accepted: 26 June 2026

Published online: 04 August 2026

Check for updates

Xin-Jian Zhang[1,2,6], Tao Deng[1,6] ✉, Nan Lin[1,6], Heng-Chang Wang[3,6], Bo Song[1,6], Er-Na Xun[4], Xian-Han Huang[1], Quan-Sheng Fu[1,2], Jun-Tong Chen[1], Peng-Rui Luo[1,2], Douglas E. Soltis[5] ✉ & Hang Sun[1] ✉

The transformation from prey to predator is a striking adaptive innovation shared by all carnivorous plants, which capture and digest diverse animal prey for nutrients (nitrogen, N). Here, we report carnivory in the alpine flowering plant *Saxifraga candelabrum* (Saxifragaceae; Saxifragales). Field experiments and herbarium surveys reveal that this plant actively attracts and captures insect prey via glandular hairs. Enzymatic analyses further confirm the ability of plants to digest prey, and isotope labelling experiments using ^{15}N-labelled insects demonstrate the transfer of nitrogen from prey to plant tissues, thus verifying the presence of carnivory. Genomic comparisons reveal a significant genome-wide convergence in genes related to carnivory (e.g., leaf morphogenesis, digestion and nutrition) across six independent origins of carnivory in diverse flowering plant lineages. Our findings provide definitive evidence of carnivory in *Saxifraga*, addressing Charles Darwin's long-standing hypothesis that some *Saxifraga* species may be capable of carnivory, and further suggest that carnivory may be more widespread among angiosperms than previously recognized.

Carnivorous plants can obtain nutrients (mainly nitrogen) by actively attracting, capturing, and ultimately digesting a diverse array of small animals, altering to some extent the predator-prey relationship between animals and plants[1,2]. Understanding how carnivory has independently arisen under physiological and ecological constraints has long fascinated biologists[3–5]. Carnivory has evolved multiple times in angiosperms, including members of 14 families[6]. Carnivorous plants are mainly placed into five major categories based on their trap type, including the widely recognized pitfall trap in pitcher plants[7,8], snap trap in Venus flytraps[9], sticky flypaper trap in sundews[10], suction trap in bladderworts, and the eel-trap or lobster-trap in corkscrew plants[11]. Despite their diverse mechanisms for trapping prey, most carnivorous plants share a common functional sequence during prey utilization, encompassing prey attraction, capture, digestion, and subsequent nutrient absorption[12].

By definition, a carnivorous plant must be capable of absorbing nutrients derived from captured animals and possess morphological, physiological, and behavioral adaptations that facilitate prey attraction, capture, digestion, and nutrient uptake[1]. Yet some plants exhibit only a subset of carnivorous traits—most commonly prey capture without clear evidence of digestion or nutrient absorption—and are therefore described as protocarnivorous[5]. This distinction underscores the need for explicit evidence to confirm true carnivory in plants. In this context, several plant lineages bearing insect-trapping

[1]State Key Laboratory of Plant Diversity and Specialty Crops & Yunnan Key Laboratory of Plant Diversity and Biogeography, Kunming Institute of Botany, Chinese Academy of Sciences, Kunming, China. [2]University of Chinese Academy of Sciences, Beijing, China. [3]State Key Laboratory of Plant Diversity and Specialty Crops, Wuhan Botanical Garden, Chinese Academy of Sciences, Wuhan, China. [4]College of Life Sciences, Jishou University, Jishou, China. [5]Florida Museum of Natural History, University of Florida, Gainesville, FL, USA. [6]These authors contributed equally: Xin-Jian Zhang, Tao Deng, Nan Lin, Heng-Chang Wang, Bo Song. ✉e-mail: dengtao@mail.kib.ac.cn; dsoltis@ufl.edu; sunhang@mail.kib.ac.cn

structures have remained controversial with respect to their carnivorous status.

The carnivorous lifestyle, long debated as representing either an herbivore defense strategy or a cost-benefit model of adaptation to nutrient-poor soils[13,14], may be more widespread among angiosperms than previously recognized[5,15]. Among the putative carnivorous lineages, *Saxifraga* L. is a predominantly north temperate genus, including species notable for sticky glandular trichomes and many members that thrive in nutrient-poor habitats such as exposed rock outcrops and crevices[4,16,17]. Inspired by his work on carnivory in *Drosera*, Darwin (1875) proposed that two *Saxifraga* species (*S. rotundifolia* and *S. umbrosa*) might similarly exhibit carnivorous behavior. Darwin regarded these two species as representing one of the most intriguing cases among plants with glandular hairs[2]. Although Darwin attempted to test this hypothesis through feeding experiments, these early attempts did not yield conclusive results[2]. The lack of conclusive evidence has prevented researchers from classifying these *Saxifraga* species as true carnivorous plants[4]. Here we revisit this long-standing hypothesis by examining possible carnivory in *Saxifraga*.

Saxifraga candelabrum Franch. is a monocarpic perennial herb mainly distributed in the alpine areas of the Qinghai-Tibet Plateau-Hengduan Mountains[18]. The species occurs from central to northern Yunnan, as well as in southwest Sichuan at an altitude of 2500–3300 m. It grows in nutrient-poor rock crevices in sunny and seasonally dry environments. The plant forms a basal rosette and bears inflorescence stems and branches covered with well-developed glandular hairs that frequently trap small insects (Figs. 1 and 2). These hairs secrete viscous secretions similar to those in other sticky flypaper trap carnivorous plants[4,19]. Although *S. candelabrum* is geographically and phylogenetically distinct from the two *Saxifraga* species discussed by Darwin, his original hypothesis was motivated by the functional properties of glandular hairs observed in those two *Saxifraga* species. It is also noteworthy that a number of species of *Saxifraga* have sticky glandular hairs. The shared presence of well-developed glandular hairs capable of trapping insects represents the key morphological and functional feature that motivated Darwin's experiments and renders *S. candelabrum* a suitable system for testing this long-standing hypothesis using modern approaches.

To investigate the potential status of *S. candelabrum* as a carnivorous plant (Fig. 1), we test the four key criteria required to confirm carnivory (prey attraction, capture, digestion, and nutrient uptake). Specifically, we address the following questions: (1) Does the plant actively attract and capture insect prey? (2) Can it directly digest prey and absorb derived nutrients? (3) Does it exhibit convergent genomic signatures with other carnivorous lineages[20]? In contrast to previous studies showing that carnivorous plants grow mainly in wetlands and swamps[3], our study focuses on a putative sticky flypaper trap carnivorous lineage from a highland ecosystem (Figs. 2 and 3). We also provide evidence of possible convergence in the genomic signature of carnivory across several diverse carnivorous plant lineages.

Results and discussion

Active prey attraction and capture

Field observations and herbarium specimen analyses show that gnats belonging to several genera (e.g., *Polypedilum*, *Chironomus*, *Cricotopus*, *Dicrotendipes*, and *Paratanytarsus*) of the family Chironomidae were the main insect visitors found trapped by glandular hairs of *Saxifraga candelabrum* (all insects identified by entomologists; Supplementary Data 1). In contrast, species from Calliphoridae, Muscidae, Syrphidae, Sarcophagidae, Colletidae, and Halictidae were the main uncaptured flower-visiting (potential pollinator) insects (Supplementary Data 1, Fig. S1). Field observations demonstrated that the number of insects trapped on *S. candelabrum* individuals correlated positively with both the number (Spearman's rank correlation $\rho = 0.38$, $n = 30$, $p = 0.038$) and length (Spearman's rank correlation $\rho = 0.33$, $n = 92$, $p = 0.001$) of inflorescence branches (Fig. 4). Juvenile plants with only a few branches exhibited minimal or no insect trapping. In contrast, mature individuals harbored an average of 71 trapped insects, predominantly localized on the glandular hairs of inflorescence branches, with significantly fewer occurrences observed on stems. This observed correlation suggested that the increased number and length of inflorescence branches may enhance insect attraction and provide a larger surface area bearing glandular hairs, potentially increasing the probability of insect capture.

In addition, examination of all available flowering herbarium specimens of *S. candelabrum* revealed that insect prey were present on glandular hairs in the vast majority of specimens (43 out of 45), spanning both the geographical range and the entire temporal span represented in the collections (Fig. 4, Supplementary Data 2). This finding indicates that insect trapping by glandular hairs is a recurrent and widespread feature of the species, rather than a sporadic or recent phenomenon.

To test whether floral visual or olfactory attractiveness was responsible for the active attraction of insects, we conducted a field experiment in which we enclosed the flowering individuals of *S. candelabrum* either with a glass enclosure (odor-blocked) or with a white net enclosure (visual-blocked). More flower-visiting insects were observed in the visual-blocked and the untreated groups than in both the odor-blocked and the net-only control groups (Fig. 4b). The visual-blocked group showed higher visitation than the odor-blocked group (two-tailed Welch's t-test: $t(8.38) = 2.76$, $p = 0.024$, Fig. 4b), indicating an olfactory response in the active attraction of insects in *S. candelabrum*.

We further analyzed the floral volatile compounds of *S. candelabrum* using gas chromatography-mass spectrometry (GC-MS), which revealed a diverse suite of floral volatiles (Supplementary Data 3). Several compounds we identified, including β-myrcene and eucalyptol, have been reported to be involved in insect perception or attraction, suggesting that the floral scent of *S. candelabrum* contains volatiles with the potential to attract insects[21,22]. Using inflorescences to capture insects may result in a conflict with pollination in *S. candelabrum*, as *Saxifraga* also depends on insects for pollination (Fig. S1)[23]. In contrast to many carnivorous plants that spatially separate flowers and traps to reduce such conflict[24,25], here we found another strategy to balance carnivory and pollination: selectively capturing non-pollinators. The effective pollinators of *S. candelabrum* were large-bodied insects belonging to the families Calliphoridae, Halictidae, Muscidae, Syrphidae, and Tachinidae, which were rarely observed trapped by the glandular hairs of the plant. In contrast, the glandular hairs predominantly trapped smaller insect visitors, primarily species of Chironomidae, which were largely ineffective as pollinators of *S. candelabrum* (Fig. S1, Supplementary Data 1).

Prey digestion and nutrition absorption

As the most widely investigated and readily detectable enzyme in studies of carnivory, phosphatase was considered a key digestive enzyme in carnivorous plants that mobilizes nutrients from prey[26]. Most carnivorous plants display phosphatase activity in glandular cells organized into glandular hairs[26]. Following treatment with the ELF97 phosphatase substrate, yellow-green fluorescence indicative of phosphatase activity was detected in the glandular hairs of the carnivorous plants *Pinguicula primuliflora* and *S. candelabrum*. This enzymatic activity indicated that *S. candelabrum* has the capacity to directly digest trapped insects, rather than relying on alternative decomposition processes. In contrast, *S. filicaulis*, a closely related and often sympatric species of *S. candelabrum* in Shangri-La, Yunnan, China, showed no detectable fluorescence under identical conditions, consistent with the observation that its glandular hairs rarely captured insects (Fig. 5).

https://doi.org/10.1038/s41467-026-75288-y

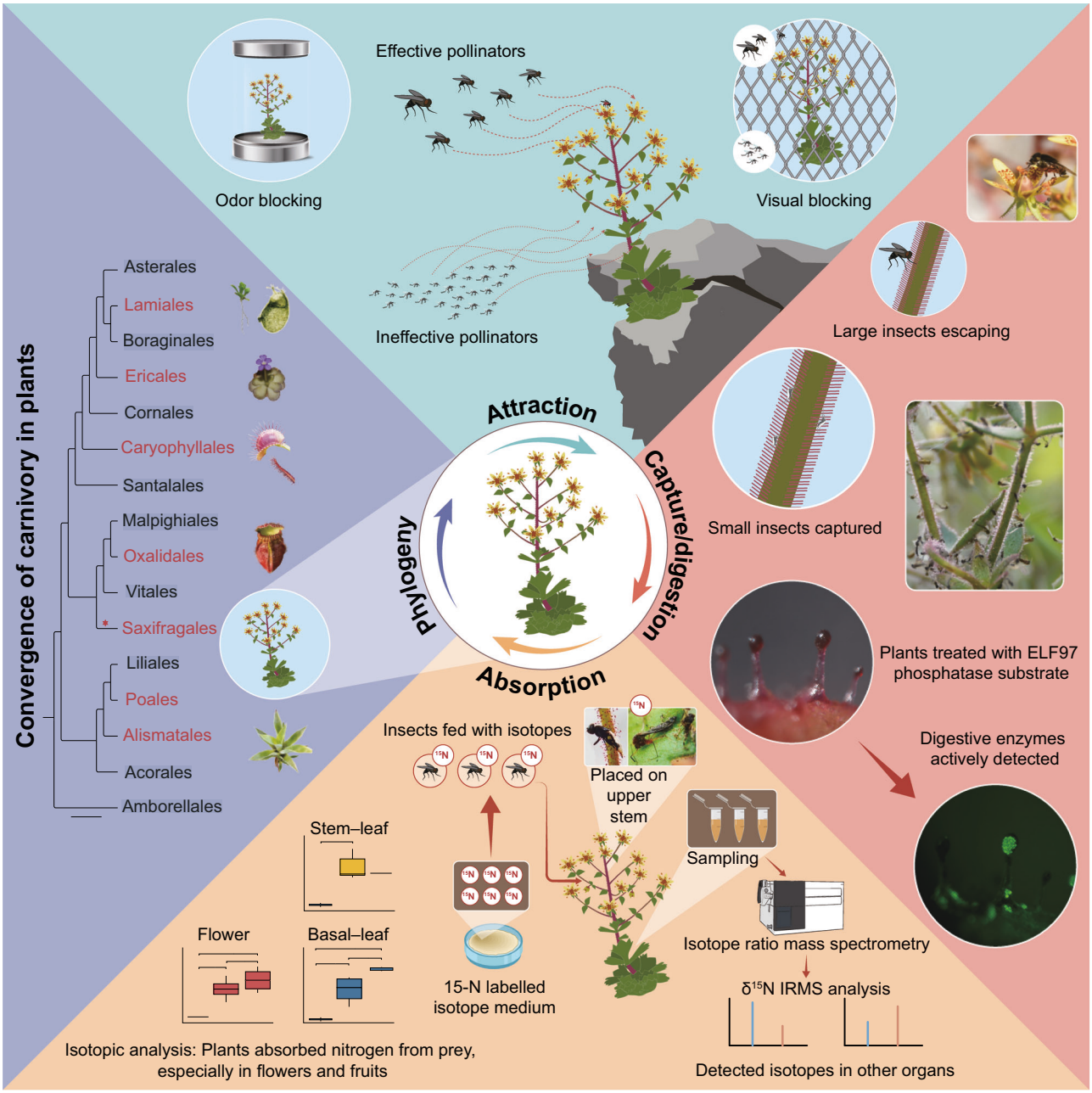

Fig. 1 | Multiple lines of evidence for carnivory in *Saxifraga candelabrum*. Phylogenetic convergence and key processes of prey attraction, capture, digestion, and absorption, supported by field experiments, enzymatic assays, and stable isotope labeling. ^{15}N denotes a stable nitrogen isotope.

In our isotopic investigation, we examined *S. candelabrum* and the distantly related carnivorous flypaper trap plant *Drosera peltata* (Droseraceae) along with two non-carnivorous sympatric species: *Salvia przewalskii* (Lamiaceae) and *Saxifraga diversifolia*. All samples used for interspecific comparisons were collected from the same locality (Wufeng Mountain, Shangri-La), although minor microhabitat differences were present within the site, as reflected by variation in natural $\delta^{15}N$ values of local soils (Supplementary Data 4), with negative control species exhibiting higher baseline $\delta^{15}N$ values than *S. candelabrum* and *D. peltata* (Fig. 6a). Application of ^{15}N-labeled *Drosophila* to *S. diversifolia*, *S. candelabrum*, *D. peltata* and *S. przewalskii* revealed no significant change of $\delta^{15}N$ in the non-carnivores *S. przewalskii* (two-tailed Welch's *t*-test: $t(7.64) = 0.03$, $p = 0.978$) and *S. diversifolia* (two-tailed Welch's *t*-test: $t(3.56) = 0.20$, $p = 0.853$) (Fig. 6, Supplementary Data 4). In contrast, $\delta^{15}N$ showed a significant increase in *D. peltata* (two-tailed Welch's *t*-test: $t(4.00) = 4.75$, $p = 0.009$) and *S. candelabrum* (two-tailed Welch's *t*-test: $t(10.10) = 5.86$, $p = 0.0001$) (Fig. 6, Supplementary Data 4). The absence of isotopic enrichment in the non-carnivorous controls indicated that the observed signal in *S. candelabrum* cannot be explained by passive absorption or surface contamination alone.

We further compared the $\delta^{15}N$ enrichment in different organs of *S. candelabrum* and found the highest $\delta^{15}N$ enrichment in flowers, followed by cauline leaves, with the lowest $\delta^{15}N$ enrichment in basal leaves (Fig. 6, Supplementary Data 4). The higher content of ^{15}N accumulated in reproductive organs than vegetative organs could not be fully explained by their proximity to glandular trichomes that absorb ^{15}N, given that cauline leaves, which were similarly close to the nitrogen sources, exhibited lower ^{15}N levels. This contrast indicated that plants actively allocate more nitrogen to their reproductive organs, a strategy that optimizes resource use to maximize reproductive output of this monocarpic plant.

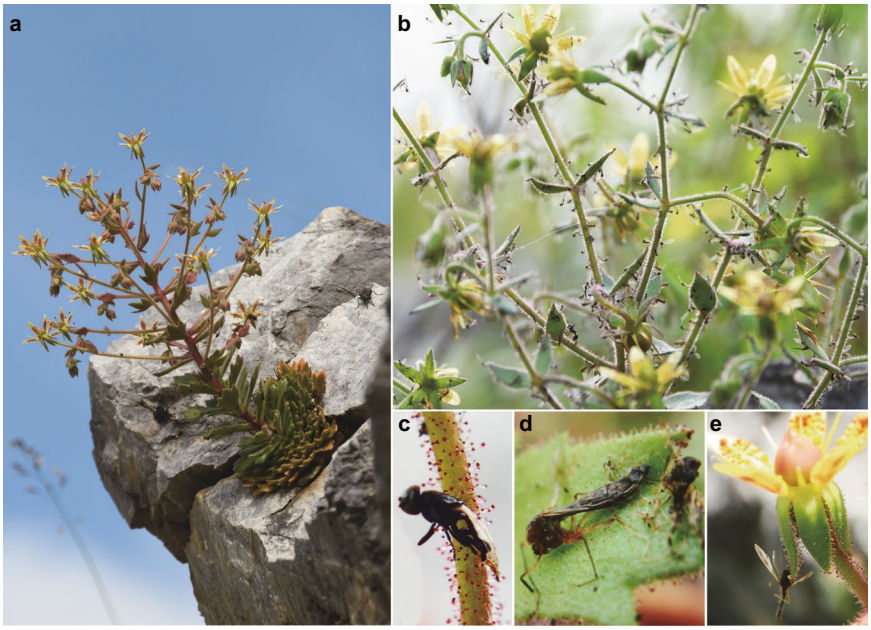

Fig. 2 | Morphology of *Saxifraga candelabrum*. **a** Flowering plants thriving in stone crevices. **b** Plants covered by insect prey. **c** Erect scape; close up of rachis. **d** Leaf with insect prey. **e** Calyx and pedicel. These photos (especially **c**–**e**) show the sticky reddish glandular hairs and captured insect prey on different parts of the plant.

To rule out ^{15}N-labeled nutrient uptake from soil, we measured δ^{15}N in soil around treated individuals. Soil δ^{15}N remained low across all treatments (Fig. 6), confirming that the δ^{15}N enrichment in *S. candelabrum* was not from the soil. The decline in δ^{15}N enrichment from 2 weeks to 20 days likely reflects the complete absorption of the limited labeled prey (10 fruit flies) within the first 2 weeks (Fig. 6), after which unlabeled soil nitrogen continued to be incorporated, diluting the isotopic signal.

Comparative genomics and carnivory

To investigate the genomics of carnivorous plants, we generated a chromosome-scale annotated genome for *S. candelabrum* (Figs. S2–S4; Supplementary Data 5–15). Our broad comparative analysis included: (1) available genomes of other Saxifragales (Supplementary Data 5; all non-carnivorous); (2) representative rosid lineages (e.g., Brassicales, Celastrales, Cucurbitales, Fabales, Fagales, Malpighiales, Myrtales, Rosales, Sapindales, Vitales: see Fig. S3); and (3) carnivorous species with flypaper traps (*Drosera spatulata*, Droseraceae; *Roridula gorgonias*, Roridulaceae), as well as other trap types, including pitcher traps (*Cephalotus follicularis*, Cephalotaceae; *Nepenthes gracilis*, Nepenthaceae), and snap traps (*Aldrovanda vesiculosa*, Droseraceae). We investigated gene family expansions, molecular convergence across independently evolved carnivorous lineages, signatures of positive selection, and assessed gene family downsizing.

Comparative genomic analysis of *S. candelabrum* and two distantly related sticky trap species (*D. spatulata*, Droseraceae; *R. gorgonias*, Roridulaceae) revealed 20 expanded gene families shared by all three sticky flypaper trap carnivorous lineages (Fig. 3; Supplementary Data 16). These shared genes were functionally enriched for key carnivorous traits, including prey attraction (GO:0009836, fruit ripening, climacteric)[27], digestion (GO:0016788, hydrolase activity)[3,9], and nutrient absorption (GO:0006817, phosphate ion transport)[12].

No common gene expansions were found across all six examined carnivorous species representing a diversity of trap types. Further pairwise comparisons between *S. candelabrum* and each carnivorous species identified additional gene family expansions associated with distinct stages of the hunting cycle, from prey attraction and capture to digestion and nutrient absorption (Fig. S5; Supplementary Data 17–21), demonstrating putatively convergent evolutionary pathways in the genomic underpinnings of plant carnivory[28–31].

Comparative genomic analysis of three distantly related carnivorous species with sticky traps (*S. candelabrum*, Saxifragaceae; *D. spatulata*, Droseraceae; *R. gorgonias*, Roridulaceae), revealed 53 genes exhibiting convergent evolutionary rate acceleration (Supplementary Data 22). Functional annotation demonstrated significant enrichment in key aspects of carnivory: (1) mucilage production and secretion (GO:0048193, Golgi vesicle transport)[31]; (2) amino acid biosynthesis (GO:0009086, methionine biosynthetic processes; GO:0009088, threonine biosynthetic process; GO:0009097, isoleucine biosynthetic processes)[32]; and (3) protein transport (GO:0043328, protein transport to vacuole)[12].

Expanding our comparative analysis to six carnivorous species representing diverse trap types, we identified 21 genes showing convergent acceleration across all lineages (Supplementary Data 23–28), including functionally important candidates involved in amino acid metabolism (aspartate-semialdehyde dehydrogenase: *ASADH*), prey digestion (ATP-dependent Clp protease ATP-binding subunit ClpX-like: *CLPX*), and nutrient processing (golgi SNAP receptor complex member 1: *GOSR1*).

Our selection analyses revealed strong evidence for adaptive evolution in carnivorous lineages. Specifically, we identified 16 genes under positive selection across all three sticky trap species (*S. candelabrum*, *D. spatulata*, and *R. gorgonias*; Supplementary Data 29), including genes putatively involved in digestion (proteasome subunit beta type-7: *PSMB7*) and signal transduction (germinal center kinase 1: *GCK1*). However, no genes showed a signature of positive selection across all six examined carnivorous species (Supplementary Data 30–34).

Notably, we found 59 convergent amino acid substitutions in the three flypaper trap species (Supplementary Data 35), functionally enriched for leaf morphogenesis (auxin response factor 2: *ARF2*), phosphatase activity (trehalose 6-phosphate synthase/phosphatase: *T6PS*), and nutrition absorption (nuclear transport factor 2-like: *NTF2-like*, nuclear pore complex protein Nup98: *NUP98*, ATP-binding cassette, subfamily C1: *ABCC1*).

Expanding our analysis to six species with diverse trap types revealed 58 additional genes with convergent substitutions

https://doi.org/10.1038/s41467-026-75288-y

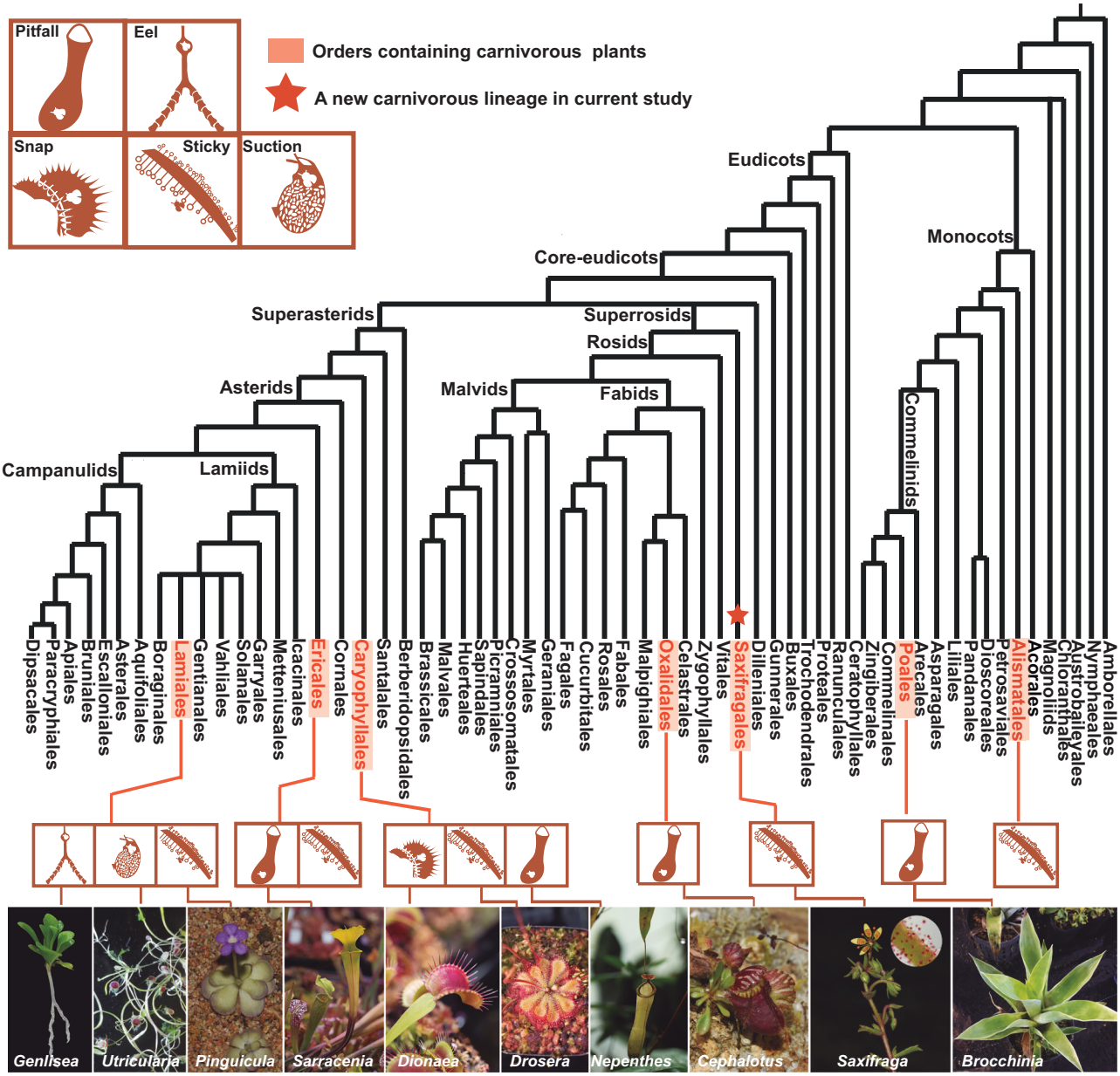

Fig. 3 | Multiple origins and trap diversity of carnivorous plants across angiosperm phylogeny. The phylogenetic framework is based on the Angiosperm Phylogeny Group IV (APG IV, 2016). Orders containing carnivorous plants are indicated on the tree. Carnivorous lineages are mapped onto major angiosperm clades, including the carnivorous lineage (*Saxifraga*) reported in this study.

(Supplementary Data 36–41), including digestive enzyme genes (CTD phosphatase-like 4: *CPL4*, a homolog of the papain family cysteine proteases: *CPs*, one homolog of the glycosyl hydrolase family 10: *GH_10*). These findings reinforce the suggestion that convergent evolution of digestive enzymes in carnivorous plants likely reflects strong selective pressures associated with alternative nutritional strategies[29,33–35].

Among the three sticky-trap species (*S. candelabrum*, *D. spatulata*, and *R. gorgonias*), we identified two convergently contracted gene families involved in cellular plasticity (GO:0030042, actin filament depolymerization), and hormone signaling (GO:0009873, ethylene-activated signaling pathway; Supplementary Data 42–45). No gene families were observed to contract across all six examined carnivorous species. Our exploration of shared gene losses in carnivorous plants revealed putative convergence of function in three key areas (Supplementary Data 46): root development (including *RCP2* and *RID3*), kinetochore formation (*H2B*-related genes and *MDC1-like*)[36–38], and photosynthesis (*CA* and *NAD(P)H*-quinone oxidoreductase)[39]. While these patterns imply potential associations, further functional studies are needed to test whether these gene losses causally underlie carnivorous adaptations.

Concluding remarks

Over a century after Darwin proposed that some *Saxifraga* species might be carnivorous[2], this study provides a clear answer. *Saxifraga candelabrum* is shown to secrete digestive enzymes and assimilate nutrients (nitrates) from captured insects, supporting its carnivorous status. This finding adds *Saxifraga*, as well as the larger order Saxifragales, to the known diversity of carnivorous plants, corroborating evidence that carnivory has arisen independently in numerous highly diverse angiosperm clades[3,19]. Our genomic analyses reveal convergence in prey-associated genes across independently evolved carnivorous lineages, while concomitantly providing candidate genes

https://doi.org/10.1038/s41467-026-75288-y

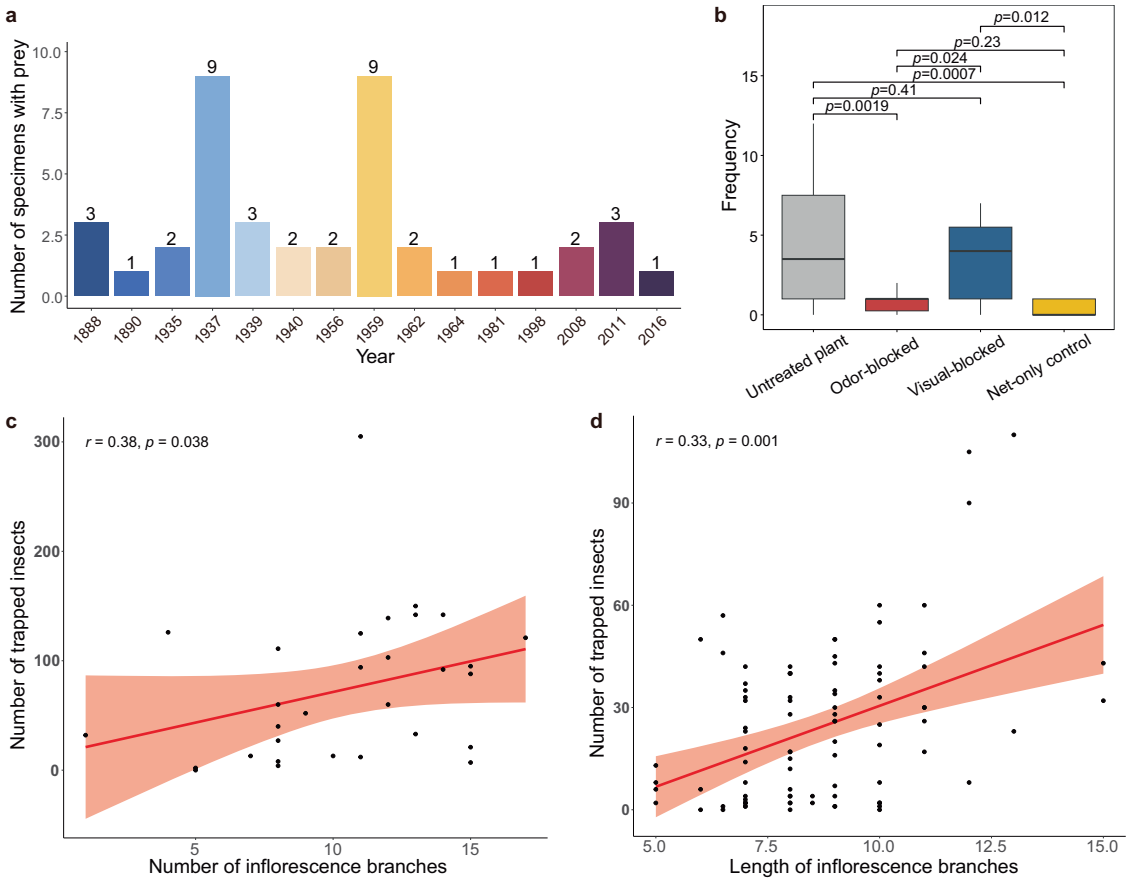

Fig. 4 | Active attraction and prey capture in *Saxifraga candelabrum*. **a** Number of herbarium specimens showing insect-trapping from 1888 to 2016. **b** Number of insect visitors to flowering individuals of *S. candelabrum* within a 10-min period under different treatments. Sample sizes: untreated ($n = 16$), odor-blocked ($n = 6$), visual-blocked ($n = 8$), and net-only control ($n = 8$); data represent independent individual plants (biological replicates). Box plots show the median (center line), the 25th and 75th percentiles (box), and whiskers extending to data points within 1.5× IQR (interquartile range) of the quartiles. Differences among treatments were tested using two-tailed Welch's *t*-tests, without adjustment for multiple comparisons. Exact *p* values are shown in the figure. **c**, **d** Field observations showing the association between the number of prey and the number (**c**) and length (**d**) of inflorescence branches, with shaded areas indicating the 95% confidence intervals around fitted regression lines. Associations were assessed using Spearman's rank correlation (two-tailed). Source data are provided as a Source Data file.

potentially involved in carnivory that should be the focus of future functional studies.

In the nutrient-poor alpine habitats where *S. candelabrum* occurs, its glandular hairs, originally used for herbivore defense[4,23], have evolved to capture small insects as prey. However, larger pollinating flies are rarely captured; these plants, therefore, appear to balance carnivory with pollination. This carnivorous adaptation to the alpine environment mirrors that seen in carnivorous plants in swamps and bogs[3]. The long-overlooked carnivory in *S. candelabrum*—despite the conspicuous glandular hairs and trapped insects—suggests the possibility of broader occurrence of carnivory not only in additional species of *Saxifraga*, but in other flowering plants. By integrating ecological and genomic approaches, this study illuminates evolutionary solutions to nutrient limitation, highlighting the role of convergent evolution in extreme environments.

Methods

Observation of insect attraction and capture

In *Saxifraga candelabrum*, insect capture occurs predominantly during the flowering (reproductive) stage, whereas only occasional insect trapping is observed during the vegetative (rosette) stage. Accordingly, insect visitors representing both uncaptured flower visitors and prey organisms trapped by glandular hairs of *S. candelabrum* were collected from flowering individuals in the field. All voucher specimens were deposited in the National Animal Collection Resource Center (NACRC) at the Institute of Zoology, Chinese Academy of Sciences, for taxonomic identification and permanent curation (Supplementary Data 1). To quantify prey capture in living plants and test the relationship between the number of trapped insects and trapping surface, we recorded the number and length of inflorescence branches, as well as the number of trapped insects on each branch, for 32 full-blooming individuals of *S. candelabrum* from Wufeng Mountain of Yunnan province in China. The relationships between the number of trapped insects and inflorescence branch number and length were assessed using Spearman's rank correlation. Linear models were used solely to visualize trends, with shaded areas indicating 95% confidence intervals.

Additionally, to assess the consistency of insect trapping across the species' geographical and temporal distribution, all available flowering specimens of *S. candelabrum* from the Herbarium of Kunming Institute of Botany, Chinese Academy of Sciences (KUN) were examined, and the number of trapped insects (prey) on glandular hairs was recorded (45 specimens spanning 1888–2016; Supplementary Data 2).

To test whether floral visual or olfactory cues attract insect visitors to *S. candelabrum* (Fig. S1), we conducted an experiment on Wufeng Mountain with the following treatments: (1) Odor-blocked: flowering individuals of *S. candelabrum* were enclosed within a transparent glass enclosure (visual attraction but no odor, with the open end of the glass enclosure sealed using transparent plastic film to minimize floral odor escape); (2) Visual-blocked: flowering individuals

https://doi.org/10.1038/s41467-026-75288-y

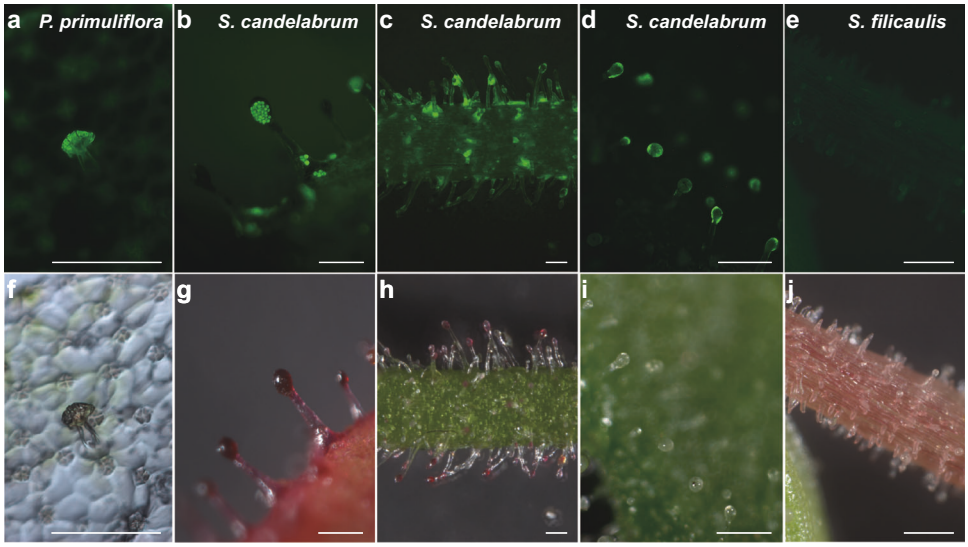

Fig. 5 | Phosphatase activity in glandular hairs was detected by ELF97 phosphatase substrate. Glandular hairs of *Pinguicula primuliflora*, *Saxifraga candelabrum*, and *Saxifraga filicaulis* stained with the ELF97 phosphatase substrate and observed under epifluorescence (**a**–**e**) and normal light microscopy (**f**–**j**). Yellow-green fluorescence indicates enzymatic hydrolysis of the phosphatase substrate. As a positive control, glandular hairs from the leaf of the carnivorous plant *P. primuliflora* show fluorescence (**a**). Fluorescence is also detected in glandular hairs of *S. candelabrum* from the sepal (**b**), stem (**c**), and leaf (**d**). In contrast, glandular hairs on the stem of the noncarnivorous species *S. filicaulis* show no apparent fluorescence (**e**, **j**). Scale bars, 200 µm. Experiments were independently repeated three times with similar results.

of *S. candelabrum* were covered with a white breathable net enclosure (permitting odor attraction); (3) Net-only control: white breathable net enclosure without *S. candelabrum* in it (testing the possibility of color attraction by the white netting); (4) Untreated: flowering individuals of *S. candelabrum* without any treatment. Each treatment included 6–16 flowering individuals of *S. candelabrum* in full bloom. Each individual was observed for 10 minutes, and the number of insect visitors was recorded during this period. Differences in the number of insect visitors among treatments were tested using two-tailed Welch's *t*-tests.

Floral volatiles collection and component analysis

The volatile compounds of *Saxifraga candelabrum* flowers were collected using the dynamic headspace sampling method[39]. Floral volatile samples were collected from three independent flowering individuals of *Saxifraga candelabrum* (SC1–SC3), each with three replicates (−1 to −3). Flowers of *S. candelabrum* were enclosed in odorless, transparent polytetrafluoroethylene (PTFE) collection bags. The air from a ventilation pump was purified through a charcoal filter, primarily to remove moisture and dust from the air. The purified air then entered the collection bag through its inlet, promoting the volatilization of floral odors inside the bag. Finally, the volatile compounds were extracted from the bag's outlet and transferred into a glass tube packed with an adsorbent. After collection, the adsorbent tube was wrapped in aluminum foil and placed in a sealed bag, then stored in a deep-freezer box and transported to the laboratory. Three non-flowering *S. candelabrum* individuals were used as controls to distinguish floral volatiles from environmental and non-floral sources.

Adsorbent tubes were eluted with 2 mL of *n*-hexane, and 0.5 mL of the eluted solution containing floral volatiles was collected in a 2 mL amber vial. The solution was concentrated to 100 µL by nitrogen blowdown[39]. Finally, the sample was stored at −18 °C in a freezer until it was removed for instrumental analysis. The GC-MS technique was used to analyze the floral volatiles[39], with the NIST11 library serving as the spectral library for volatile identification, and only compounds with a match score ≥ 80 were retained (Supplementary Data 3). Analyses of the floral volatiles were performed with an Agilent 7890 gas chromatograph/5975 mass selective detector with a DB-5MS capillary column with a length of 30 m. Helium was used as the carrier gas at a constant flow rate of 1 mL/min. The oven conditions included an initial temperature of 60 °C for 1 min, the temperature increased at a rate of 10 °C/min to 130 °C, and then 6 °C/min to 250 °C for 10 min. The inlet temperature was kept constant at 250 °C, and the MS transfer line was set at 290 °C. MS acquisition parameters included scanning from *m/z* 50–600 in the electron impact (EI) mode for routine analysis. Data processing and peak identification were conducted using MSD ChemStation (Agilent Technologies, version E.02.02.1431).

Determination of enzyme activity

Inflorescence stems of field-collected *Saxifraga candelabrum* were kept intact and immersed in a solution of ELF97 phosphatase substrate (Invitrogen/Molecular Probes of Thermo Fisher Scientific)[40]. Samples were incubated in a substrate solution of 250 µM ELF97 phosphatase substrate in Milli-Q water (diluted 1:20) at room temperature for 15 min. Materials were then examined for fluorescence under an epifluorescence microscope (ZEISS Discovery V20 microscope equipped with an EBQ 100 isolated mercury lamp; excitation, 450–490 nm; dichromatic mirror, DM 510 nm; emission filter, 510 nm) at the Microscopy and Image Analysis Facility (Kunming Institute of Botany, Chinese Academy of Sciences). Fluorescence was documented using a Canon EOS Rebel T5 digital camera. Unstained samples of *S. candelabrum* were used to check for possible autofluorescence. To provide biological controls, inflorescence stems of *Pinguicula primuliflora* C.E. Wood & R.K. Godfrey (carnivorous) and *Saxifraga filicaulis* Wall. & Ser. (closely related, noncarnivorous) were processed in parallel.

Experiments for nutrient uptake

More than 1000 fruit flies (*Drosophila melanogaster*) were fed with ^{15}N-labeled amino acids for approximately two months, allowing multiple generations to develop and ensuring stable isotopic enrichment. The labeled diet was prepared by adding 100 mg algal amino acid mixture (Sigma-Aldrich, 98 atom%^{15}N) to 100 g standard *Drosophila* medium. Another 500 fruit flies were fed with normal standard *Drosophila* medium as a control[19]. Adult *Drosophila melanogaster* ($n = 12$) were randomly selected and weighed individually using an analytical balance, and the average fresh body mass was 0.403 ± 0.011 mg

https://doi.org/10.1038/s41467-026-75288-y

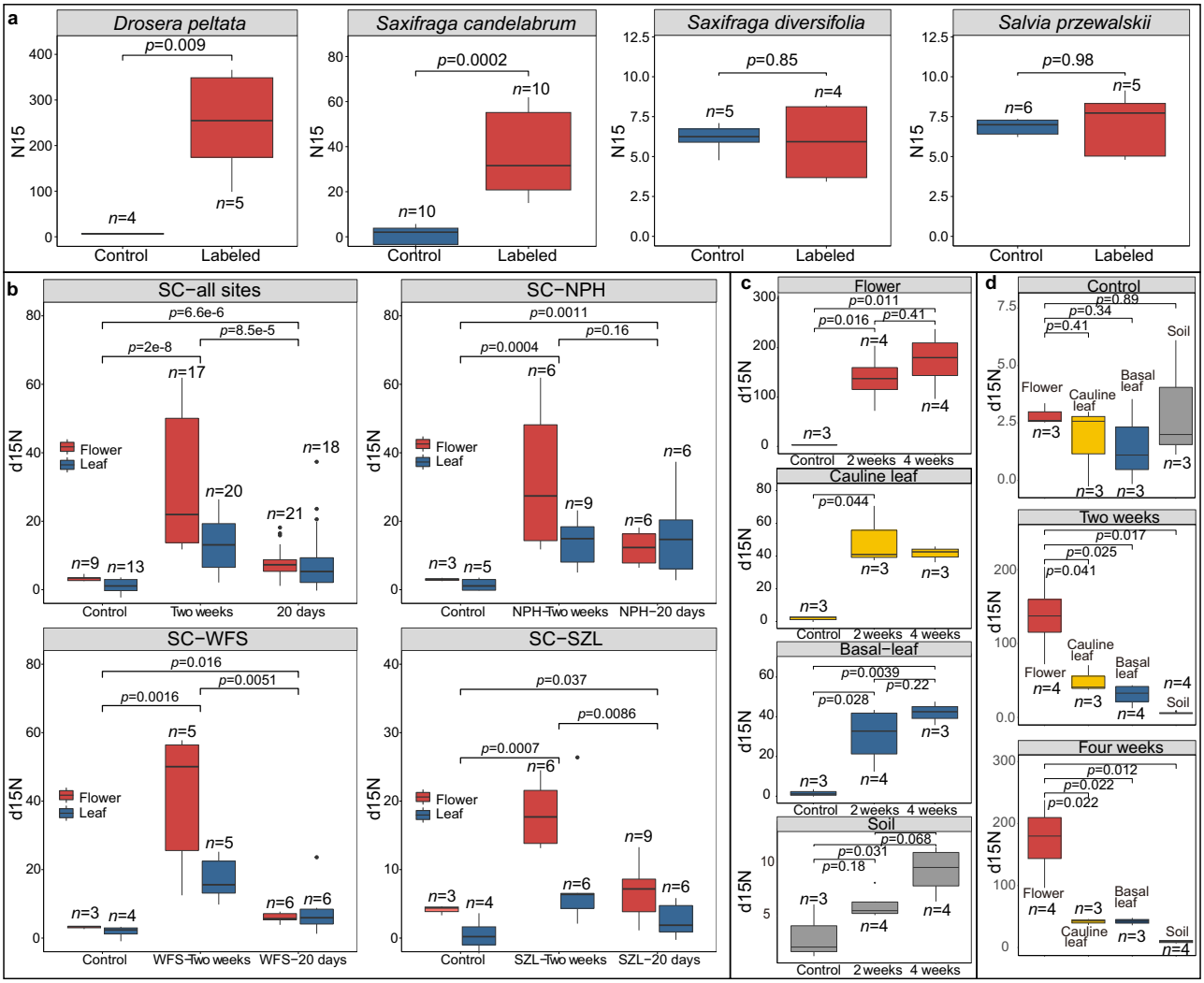

Fig. 6 | Isotopic examination of nitrogen absorption. a Changes of δ^{15}N in *Drosera peltata*, *Saxifraga candelabrum*, *Saxifraga diversifolia*, and *Salvia przewalskii* after application of ^{15}N-labeled *Drosophila*. **b** Field experiment showing changes of δ^{15}N in different organs (flower and leaf) of *S. candelabrum* from different localities after application of ^{15}N-labeled *Drosophila*. SC: *S. candelabrum*; NPH: Napahai; WFS: Wufeng Mountain; SZL: Songzanlin-Lamasery. **c** δ^{15}N enrichment in individual organs (flower, cauline leaf, basal leaf) under control, two-week labeled, and four-week labeled treatments. **d** Comparison of δ^{15}N enrichment across organs within each treatment group. In all experiments, control individuals were treated with unlabeled fruit flies for 2 weeks, whereas labeled treatments involved exposure to ^{15}N-labeled *Drosophila* for the durations indicated. Box plots show the median (center line), the 25th and 75th percentiles (box), and whiskers extending to data points within 1.5× IQR of the quartiles. Sample sizes (biological replicate) for each treatment are indicated in the corresponding panels. Differences between treatments were tested using two-tailed Welch's *t*-tests, without adjustment for multiple comparisons. Exact *p* values are shown in the figure. Source data are provided as a Source Data file.

(mean ± SD). Fruit flies were then frozen at −20 °C before the experiment. Field experiments were conducted on 60 individuals of *Saxifraga candelabrum* across three localities in Shangri-La (Wufeng Mountain, Napahai, Songzanlin-Lamasery) of Yunnan province in China. Laboratory experiments were also conducted using 20 individuals to eliminate potential environmental influences. Fruit flies were placed on the upper stems of *S. candelabrum*, *Saxifraga diversifolia* (negative control), calyces of *Salvia przewalskii* (negative control), and leaves of *Drosera peltata* (positive control). *S. diversifolia* was selected as a negative control as it is a close relative of *S. candelabrum* and, based on our observations, shows no evidence of insect capture, despite possessing glandular hairs. *Salvia przewalskii* was chosen as a control because it often co-occurs with *S. candelabrum* in Shangri-La, and has sticky glandular hairs restricted to its calyx, but no evidence of carnivory. For interspecific comparisons, *S. candelabrum*, *S. diversifolia*, *S. przewalskii*, and *D. peltata* were all sampled from the same locality (Wufeng Mountain, Shangri-La).

For the first three species noted above (*S. candelabrum*, *S. diversifolia*, *S. przewalskii*), fruit flies were gently placed on the glandular surfaces. To prevent the insects from falling off, small strips of parafilm were wrapped around the stem near the insects, following the method described by Lin et al.[19] Five to ten individuals of each species were treated with ten unlabeled fruit flies for two weeks as controls. Five to ten individuals of each species were treated with ten ^{15}N-labeled fruit flies for each treatment, and tissues were harvested two weeks after treatment for isotopic analysis. In addition, for *S. candelabrum*, additional samples were collected 20 and 28 days after treatment to examine temporal changes in prey-derived nitrogen uptake.

Stems or leaves of *D. peltata*, *S. przewalskii*, *S. candelabrum*, and *S. diversifolia* were collected and analyzed for nutrient absorption[19]. For *S. candelabrum*, the δ^{15}N of flowers, cauline leaves, and basal leaves (different plant organs from the same individuals under each treatment) were also measured. We also measured the δ^{15}N of soil around the treated *S. candelabrum* to evaluate the potential contributions

from labeled fruit flies falling into soil and being absorbed by roots. To avoid potential overestimation caused by residual labeled material remaining on glandular surfaces, the upper stems of *Saxifraga*, calyces of *Salvia*, and leaves of *D. peltata* directly exposed to labeled fruit flies were excluded from $\delta^{15}N$ measurements.

All plant samples were dried at 105 °C for 30 min, and then at 65 °C for 48 h. After that, all samples were ground into powder and sent to the Stable Isotope Facility (Kunming Biological Diversity Regional Center of Instruments, Chinese Academy of Sciences) for isotopic analysis. $\delta^{15}N$ values were measured using a Delta V Advantage mass spectrometer (Thermo Scientific) and expressed in units of per mil (‰) where $\delta = [(R_{sample}/R_{standard}) - 1] \times 1000$, $R = {}^{15}N:{}^{14}N$, with nitrogen in the air as the standard. The precision was typically ±0.3‰ for $\delta^{15}N$. Differences in $\delta^{15}N$ values among species and treatments were assessed using two-sided Welch's *t*-tests.

Genome sequencing, assembly, and assessment

Fresh basal leaves of *Saxifraga candelabrum* were collected from Wufeng Mountain, Yunnan province, China [27.820°N, 99.723°E; voucher specimen (Deng 14228) was deposited in the Herbarium of Kunming Institute of Botany, Chinese Academy of Sciences (KUN)]. Genomic DNA was extracted using standard CTAB methods[41]. The DNA quality was monitored on 1% agarose gels, while DNA purity and concentration were checked using the NanoPhotometer® spectrophotometer (Implen, CA, USA) and the Qubit 2.0 Fluorimeter (Life Technologies, CA, USA), respectively. The genome size of the sequenced *S. candelabrum* individual was estimated to be ~2.24 Gb using a k-mer approach (Fig. S2A)[42,43].

Karyotype and chromosome number determination of *S. candelabrum* were performed using root tips. Field-collected seeds were germinated on sterilized filter paper moistened with 12.5 mg/L gibberellic acid (GA) in distilled water, incubated at 20 °C with ample light. Root tips (0.3–0.5 cm) were harvested from non-detected seedlings. Root tips were pretreated with 0.002 mol/L 8-hydroxyquinoline at room temperature in darkness for 3 h to arrest metaphase, and then fixed in Carnoy's solution (3:1 ethanol: acetic acid) at 4 °C for ≥24 h. Fixed samples were hydrolyzed in 1 M HCl at 60 °C for 13 min, rinsed in distilled water, and stained with 20–25% acetocarmine for ≥24 h. Stained root tips were squashed on slides under a coverslip and observed using an Olympus BX-51 microscope at 100× oil immersion. Well-spread metaphase cells were photographed with Images Advanced 3.0 software to confirm the karyotype (Fig. S2B; $2n = 2x = 16$).

Two paired-end libraries were constructed with insert sizes of 350 bp and sequenced on the Illumina NovaSeq X Plus platform (Illumina, San Diego, CA, USA). For the long-read sequencing, third-generation sequencing 20-kb libraries were constructed and sequenced using the PacBio HiFi platform (Pacific Biosciences, Menlo Park, CA, USA) according to the manufacturer's protocol. For the Hi-C technology, fresh young leaves of *S. candelabrum* (Deng14228) were preserved in liquid nitrogen for library construction. This process involved chromatin extraction, digestion, ligation, fragmentation, and followed by sequencing on an Illumina NovaSeq X Plus platform. Raw reads from Illumina sequencing were filtered using fastp v0.21.0[44], while quality control of third-generation data was performed using SMRT Link v11.0 and CCS v6.0.0 software[45,46]. For Hi–C data quality control, reads were filtered using fastp v0.21.0, and HICUP v0.8.0 was performed for further filtering[47]. Accordingly, a total of 117.32 Gb (~58×) clean PacBio long reads were utilized for genome assembly with Hifiasm v0.16.1 (Supplementary Data 5–7)[48]. The preliminary de novo assembly with PacBio long reads contained 770 contigs with a total length of 2.09 Gb (contig N50 = 10.21 Mb). To anchor these contigs to chromosomes, 372.75 Gb (~186×) Hi–C clean reads were aligned to the draft reference genome using ALLHiC v0.9.8 to assist in genome assembly through clustering, ordering, and orienting scaffolds onto chromosomes[49].

Visualization of the genome maps was achieved using Juicebox v1.11.08[50]. According to the strength of chromosome interaction, 98.56% of the initial de novo assembly contig sequences were then anchored to a model of 8 pseudochromosomes based on ALLHiC v0.9.8, being consistent with the chromosome number result (Fig. S2B-D). With the integration of Hi-C data, the outassembled genome size was finalized at 2.086 Gb, with scaffold N50 reaching 232.01 Mb. Finally, Illumina paired-end reads were mapped to the assembled genome to evaluate the accuracy of the genome assembly using the Burrows-Wheeler Aligner (BWA) v0.7.12-r1039[51]. Illumina paired-end reads mapping rate exceeded 99.77%, indicating a nearly complete assembled genome (Supplementary Data 8–10). The completeness of the genome assembly was assessed using Benchmarking Universal Single-Copy Orthologs (BUSCO) v4.0.5[52], which showed that 95.4% of 1539 genes were found in the *S. candelabrum* genome (Supplementary Data 11).

Gene repeats and genome annotation

Both de novo prediction and homologous alignment were used to detect repeated sequences. RepeatModeler v1.0.11 was used to build the repeat sequence database[53], LTR_FINDER v1.0.7[54], and LTR_retriever v2.8 were used for de novo estimation[55]. RepeatMasker and RepeatProteinMask programs were then used to conduct homologous sequence alignment by searching the RepBase database[56]. For the ncRNA, transfer RNAs (tRNAs) were predicted using tRNAscan-SE v1.23[57]. The rRNAs and their subunits were predicted using the rRNA database. MicroRNA, small nuclear RNA, and small nucleolar RNA were identified using INFERNAL v1.1.2 to search the Rfam database[58]. As a result, repetitive sequences accounted for 84.20% of the whole-genome size (Supplementary Data 12), which was highly similar to the results of the k-mer distribution analysis (83.54%). Long terminal repeat retrotransposons (LTR-RTs) constituted the largest portion of repetitive sequences (76.17%).

Three independent strategies, including ab initio prediction, homology search, and reference-guided transcriptome assembly, were used for gene prediction. For de novo prediction, AUGUSTUS v3.3.2 and GlimmerHMM v3.04 were utilized for ab initio gene prediction[59,60]. For RNA-seq-based gene prediction, RNA was extracted using an RNAprep Pure Plant Kit (Tiangen Biotech, Beijing, China) from the roots, stems, flowers, and leaves of *Saxifraga candelabrum,* and RNA was used to produce cDNA for transcript sequencing on an Illumina NovaSeq X Plus platform (Illumina, San Diego, CA, USA). For homology searches, Blast v2.7.1 was used to align the homologous peptides from four species (i.e., *Arabidopsis thaliana*, *Sedum album*, *Aldrovanda vesiculosa,* and *Drosera spatulata*) and Exonerate v2.4.0 was employed for coding region prediction and the gene structure information[61,62]. The predicted results were integrated using the MAKER v2.31.10 and were ensured by combining evidence[63]. After gene prediction, gene function information, motifs, and domains were assigned by comparisons with public databases with an E-value cut-off of 1e − 5, including Gene Ontology (GO), Kyoto Encyclopedia of Genes and Genomes (KEGG)/EuKaryotic Orthologous Groups (KOG), UniProt, and NCBI nonredundant protein (NR) databases. Ultimately, 42,143 (88.63%) from the 47,550 annotated genes showed functional evidence from combined evidences (Supplementary Data 13–14).

Gene family identification and phylogenetic analysis

A total of 31 species were investigated in a broad phylogenomic analysis to construct orthogroups using OrthoFinder v2.4 (Fig. S3; Supplementary Data 5)[64]. We included *Saxifraga candelabrum* and six representative species from Saxifragales for which published genomic data are available (Crassulaceae: *Kalanchoe fedtschenkoi*, *Kalanchoe marnieriana*, *Sedum album,* and *Rhodiola crenulata*; Altingiaceae: *Liquidambar formosana*; Saxifragaceae: *Tiarella polyphylla*)[65–69]. At a broader scale we used 15 representative species from various rosids clades (Brassicales: *Arabidopsis thaliana*; Celastrales: *Tripterygium*

wilfordii; Cucurbitales: *Cucumis sativus*; Fabales: *Trifolium pratense*, *Vigna radiata*; Fagales: *Juglans regia*, *Morella rubra*; Malpighiales: *Linum usitatissimum*; *Populus trichocarpa*; Myrtales: *Corymbia citriodora*; Sapindales: *Citrus maxima*; Rosales: *Morus notabilis*, *Prunus avium*, *Prunus persica*; Vitales: *Vitis vinifera*)[70–84], five available representative carnivorous species (Caryophyllales: *Aldrovanda vesiculosa*, *Drosera spatulata*, *Nepenthes gracilis*; Oxalidales: *Cephalotus follicularis*; Ericales: *Roridula gorgonias*)[85–88], two non-carnivorous species in Caryophyllales (*Amaranthus hypochondriacus* and *Spinacia oleracea*)[89,90] and two outgroup species representing the monocots and basal angiosperms, respectively (Poales: *Zea mays*; Nymphaeales: *Nymphaea colorata*)[91,92].

For the identification of gene families among these 31 species, we used OrthoFinder v2.4[64]; protein sequences were extracted from the available genome data (Supplementary Data 5). Alternative splicing was filtered out, and only the longest transcript was retained using a Python script for gene family analysis of each species. The similarities between protein sequences were calculated based on an all-vs-all BLAST with an E-value threshold of 1e − 3. In total, 64,092 orthogroups were identified among all of the 31 species (Fig. S4, Supplementary Data 15).

Four-fold synonymous (degenerative) third-codon transversion (4DTv) and synonymous substitution rates (Ks) methods were performed to search for putative WGD events[93]. LTR_FINDER v1.0.7 was used to search for LTR sequences[54], and LTR_retriever v2.8 was used to filter out redundant LTR sequences to obtain accurate LTR sequences[55]. The flanking sequences on both sides of each LTR were extracted and compared to MAFFT v7.30 (parameters: --localpair), and EMBOSS v6.6.0 was used to estimate the distance (k) between the two sides in terms of the Kimura model[94,95]. The $t = k/(2 \times r)$ was used to estimate the divergent time with the molecular clock (Fig. S5; $r = 7 \times 10^{-9}$).

Convergent gene family evolution

Gene family expansion and contraction were investigated with CAFÉ v4.2[103] using a birth and death process to model gene gain and loss based on the phylogenetic tree from OrthoFinder v2.4 of the 31 species[64]. Gene Ontology and KEGG enrichment analyses were further performed to identify significantly expanded or contracted terms using the 'clusterProfiler' package in R v4.3[96]. To further determine whether there were orthologs experiencing convergent shifts in selective pressure, especially to assess possible acceleration along branches to the carnivorous species, the 'RERconverge' package in R v4.3 was employed to estimate the relative evolutionary rate (RER) in carnivorous species[97].

Briefly, RERs are calculated as relative branch lengths by normalizing branch lengths for focal branches (i.e., carnivorous branches) across all genes. The program compares rates of change in focal foreground branches (i.e., carnivorous branches) and the remaining branches (i.e., the non-carnivorous branches), and identifies genes with a significant correlation between relative evolutionary rate and a phenotypic trait (i.e., carnivorous species). The RERs analyses only allow one gene copy per species in each gene family, but the resulting number of single-copy genes is very low, as determined by OrthoFinder v2.4, due to the distant phylogenetic relationships among some of the 31 species. Thus, we further reduced the number of orthogroups detected by OrthoFinder v2.4 with multiple gene copies per species to one copy per species. We focused our analysis on orthogroups containing at least one carnivorous species representative. Protein sequences from these filtered orthogroups were then aligned using MAFFT (v7.30)[95]. The gene trees were further constructed based on each orthogroup using RAxML v8.2.12, and only one gene copy per species was extracted according to the branch length and phylogenetic position. Finally, 3161 one-to-one genes were obtained for subsequent analyses, and protein sequences were aligned using PRANK v170427[98]. The corresponding coding sequences were further extracted based on the gene identification of the proteome sequences. For RERs analyses, the branch lengths of each gene tree of 3161 one-to-one genes were estimated using the 'phangorn' package, and RERs were further calculated for each branch of the corresponding gene tree by the 'RERconverge' package in R v4.3. The carnivorous species were set as foreground branches (i.e., carnivorous branches) to test for a significant association between RERs and phenotype (i.e., carnivorous species) across all branches of each tree with a p-value less than 0.05.

To further characterize the patterns of molecular evolution associated with carnivory, we estimated the ratio of non-synonymous to synonymous rate (dN/dS) for each carnivorous and non-carnivorous plant for each gene using a branch-site test aBSREL in HyPhy v2.5 with six convergent carnivorous plants set as foreground branches[99]. The positively selected genes were recorded when they occurred in at least three independent carnivorous species from the aBSREL results. To determine if convergent amino acid substitutions were present at specific gene sites, we identified convergent substitution sites using FADE (FUBAR Approach to Directional Evolution) in HyPhy v2.5 for each gene. FADE identifies sites experiencing directional selection towards specific amino acids in foreground relative to background branches.

For the above analyses, we first compared *Saxifraga candelabrum* to two other sticky trap species (*Drosera spatulata*, Droseraceae; *Roridula gorgonias*, Roridulaceae) to explore the molecular convergence in all three sticky flypaper trap carnivorous lineages. We further performed comparative genomic analyses across all six examined carnivorous species, including not only sticky flypaper traps (*D. spatulata*, Droseraceae; *R. gorgonias*, Roridulaceae; *S. candelabrum*, Saxifragaceae), but also pitcher traps (*Cephalotus follicularis*, Cephalotaceae; *Nepenthes gracilis*, Nepenthaceae), and snap traps (*Aldrovanda vesiculosa*, Droseraceae). Finally, pairwise comparisons between *S. candelabrum* and each carnivorous species were conducted to identify possible additional trap-specific molecular convergence associated with carnivory.

Reporting summary

Further information on research design is available in the Nature Portfolio Reporting Summary linked to this article.

Data availability

The sequencing data generated in this study, including raw data for genome assembly (PacBio HiFi reads, Illumina short reads, and Hi−C data) and genome annotation (RNA sequencing data), have been deposited in the NCBI SRA database under accession codes PRJNA1110373 and PRJNA1110349. The assembled genome of *Saxifraga candelabrum* has been deposited in the Genome Warehouse in the National Genomics Data Center under accession number GWHJIYQ00000000.1 [https://ngdc.cncb.ac.cn/gwh/Assembly/130652/show]. Raw mass spectrometry data are available in Zenodo (https://doi.org/10.5281/zenodo.19695105)[100]. Source data for Fig. 4 and Fig. 6 are provided in the Source Data file. Supplementary Data 1–47 are provided in Supplementary Data file. Previously published genomic datasets used in this study are available in publicly accessible repositories, and their accession numbers are provided in Supplementary Data 47. All other data supporting the findings of this study are available within the paper and its Supplementary Information. Source data are provided with this paper.

Code availability

R scripts and related source data used for statistical analyses and figure generation in this study are available in Zenodo (https://doi.org/10.5281/zenodo.20322891)[101]. Scripts used for genome-based convergence analyses are available at Zenodo (https://doi.org/10.5281/zenodo.20411937)[102].

References

1. Givnish, T., Burkhardt, E., Happel, R. & Weintraub, J. Carnivory in the bromeliad *Brocchinia reducta*, with a cost/benefit model for the general restriction of carnivorous plants to sunny, moist, nutrient-poor habitats. *Am. Nat.* **124**, 479–497 (1984).
2. Darwin, C. *Insectivorous Plants* (John Murray, 1875).
3. Hedrich, R. & Fukushima, K. On the origin of carnivory: Molecular physiology and evolution of plants on an animal diet. *Annu. Rev. Plant Biol.* **72**, 133–153 (2021).
4. Chase, M., Christenhusz, M., Sanders, D. & Fay, M. Murderous plants: Victorian Gothic, Darwin and modern insights into vegetable carnivory. *Bot. J. Linn. Soc.* **161**, 329–356 (2009).
5. Givnish, T., Sparks, K., Hunter, S. & Pavlovič, A. in *Carnivorous Plants: Physiology, Ecology, and Evolution*, (eds A. M. Ellison, L. Adamec) (Oxford University Press, 2018), pp 232–255.
6. Soltis, D. et al. *Phylogeny and Evolution of the Angiosperms* (University of Chicago Press, 2018).
7. Thorogood, C., Bauer, U. & Hiscock, S. Convergent and divergent evolution in carnivorous pitcher plant traps. *N. Phytol.* **217**, 1035–1041 (2018).
8. Chomicki, G. et al. Convergence in carnivorous pitcher plants reveals a mechanism for composite trait evolution. *Science* **383**, 108–113 (2024).
9. Poppinga, S., Kampowski, T., Metzger, A., Speck, O. & Speck, T. Comparative kinematical analyses of Venus flytrap (*Dionaea muscipula*) snap traps. *Beilstein J. Nanotechnol.* **7**, 664–674 (2016).
10. Gibson, T. & Waller, D. Evolving Darwin's 'most wonderful' plant: ecological steps to a snap-trap. *N. Phytol.* **183**, 575–587 (2009).
11. Westermeier, A. et al. How the carnivorous waterwheel plant (*Aldrovanda vesiculosa*) snaps. *Proc. R. Soc. B* **285**, 20180012 (2018).
12. Palfalvi, G. et al. Genomes of the Venus flytrap and close relatives unveil the roots of plant carnivory. *Curr. Biol.* **30**, 2312–2320 (2020).
13. Roberts, H., Warren, J. & Provan, J. New evidence on the origin of carnivorous plants. *Proc. Natl. Acad. Sci. USA* **112**, 10–11 (2015).
14. Ellison, A. & Adamec, L. Ecophysiological traits of terrestrial and aquatic carnivorous plants: are the costs and benefits the same?. *Oikos* **120**, 1721–1731 (2011).
15. Darnowski, D., Carroll, D., Plachno, B., Kabanoff, E. & Cinnamon, E. Evidence of protocarnivory in triggerplants (*Stylidium* spp.; Stylidiaceae). *Plant Biol.* **8**, 805–812 (2006).
16. Xu, B., Li, Z. & Sun, H. *Seed plants of the alpine subnival belt from the Hengduan Mountains, SW China* (Science Press, 2013).
17. Ebersbach, J., Schnitzler, J., Favre, A. & Muellner-Riehl, A. Evolutionary radiations in the species-rich mountain genus *Saxifraga* L. *BMC Evol. Biol.* **17**, 119 (2017).
18. Pan, J., Gornall, R. & Ohba, H. Saxifragaceae. in *Flora of China*, (eds C. Y. Wu, P. H. Raven) (Science Press and Missouri Botanical Garden Press, 2001), vol. 8, pp 280–344.
19. Lin, Q., Ane, C., Givnish, T. & Graham, S. A new carnivorous plant lineage (*Triantha*) with a unique sticky-inflorescence trap. *Proc. Natl. Acad. Sci. USA* **118**, e2022724118 (2021).
20. Pereira, C. et al. Underground leaves of *Philcoxia* trap and digest nematodes. *Proc. Natl. Acad. Sci. USA* **109**, 1154–1158 (2012).
21. Dötterl, S. & Gershenzon, J. Chemistry, biosynthesis and biology of floral volatiles: roles in pollination and other functions. *Nat. Prod. Rep.* **40**, 1901–1937 (2023).
22. Perkins, J., Hayashi, T., Peakall, R., Flematti, G. R. & Bohman, B. The volatile chemistry of orchid pollination. *Nat. Prod. Rep.* **40**, 819–839 (2023).
23. Bemm, F. et al. Venus flytrap carnivorous lifestyle builds on herbivore defense strategies. *Genome Res.* **26**, 812–825 (2016).
24. Ellison, A. & Adamec, L. in *Carnivorous Plants: Physiology, Ecology, and Evolution*, (eds Ellison, A. & Adamec, L.) (Oxford University Press, 2018), pp 3–6.
25. Ellison, A. & Gotelli, N. Evolutionary ecology of carnivorous plants. *Trends Ecol. Evol.* **16**, 623–629 (2001).
26. Plachno, B., Adamec, L. & Huet, H. Mineral nutrient uptake from prey and glandular phosphatase activity as a dual test of carnivory in semi-desert plants with glandular leaves suspected of carnivory. *Ann. Bot.* **104**, 649–654 (2009).
27. Rodriguez, A., Alquezar, B. & Pena, L. Fruit aromas in mature fleshy fruits as signals of readiness for predation and seed dispersal. *N. Phytol.* **197**, 36–48 (2013).
28. Fukushima, K. et al. Oriented cell division shapes carnivorous pitcher leaves of *Sarracenia purpurea*. *Nat. Commun.* **6**, 6450 (2015).
29. Freund, M. et al. The digestive systems of carnivorous plants. *Plant Physiol.* **190**, 44–59 (2022).
30. Fukushima, K. et al. Genome of the pitcher plant *Cephalotus* reveals genetic changes associated with carnivory. *Nat. Ecol. Evol.* **1**, 59 (2017).
31. Outenreath, R. & Dauwalder, M. Ultrastructural and radioautographic studies of the digestive gland cells of *Drosera capensis* I. development and mucilage secretion. *J. Ultrastruct. Res.* **80**, 71–88 (1982).
32. Kováčik, J. et al. Prey-induced changes in the accumulation of amino acids and phenolic metabolites in the leaves of *Drosera capensis* L. *Amino Acids* **42**, 1277–1285 (2012).
33. Pavlovic, A. & Saganova, M. A novel insight into the cost-benefit model for the evolution of botanical carnivory. *Ann. Bot.* **115**, 1075–1092 (2015).
34. Lan, T. et al. Long-read sequencing uncovers the adaptive topography of a carnivorous plant genome. *Proc. Natl. Acad. Sci. USA* **114**, E4435–E4441 (2017).
35. Scherzer, S. et al. Insect haptoelectrical stimulation of Venus flytrap triggers exocytosis in gland cells. *Proc. Natl. Acad. Sci. USA* **114**, 4822–4827 (2017).
36. Adlassnig, W. et al. The roots of carnivorous plants. *Plant Soil* **274**, 127–140 (2005).
37. Wicke, S., Schäferhoff, B., dePamphilis, C. & Müller, F. Disproportional plastome-wide increase of substitution rates and relaxed purifying selection in genes of carnivorous Lentibulariaceae. *Mol. Biol. Evol.* **31**, 529–545 (2014).
38. Kolodin, P. et al. Holocentric chromosomes may be an apomorphy of Droseraceae. *Plant Syst. Evol.* **304**, 1289–1296 (2018).
39. Tholl, D. et al. Practical approaches to plant volatile analysis. *Plant J.* **45**, 540–560 (2006).
40. Nedoma, J., Strojsová, A., Vrba, J., Komárková, J. & Simek, K. Extracellular phosphatase activity of natural plankton studied with ELF97 phosphate: fluorescence quantification and labelling kinetics. *Environ. Microbiol.* **5**, 462–472 (2003).
41. Doyle, J. J. & Doyle, J. L. A rapid DNA isolation procedure for small quantities of fresh leaf tissue. *Phytochem. Bull.* **19**, 11–15 (1987).
42. Ranallo-Benavidez, T. R., Jaron, K. S. & Schatz, M. C. GenomeScope 2.0 and smudgeplot for reference-free profiling of polyploid genomes. *Nat. Commun.* **11**, 1432 (2020).
43. Marcais, G. & Kingsford, C. A fast, lock-free approach for efficient parallel counting of occurrences of k-mers. *Bioinformatics* **27**, 764–770 (2011).
44. Chen, S., Zhou, Y., Chen, Y. & Gu, J. fastp: an ultra-fast all-in-one FASTQ preprocessor. *Bioinformatics* **34**, i884–i890 (2018).
45. Koren, S. et al. De novo assembly of haplotype-resolved genomes with trio binning. *Nat. Biotechnol.* **36**, 1174–1182 (2018).
46. Korlach, J. et al. De novo PacBio long-read and phased avian genome assemblies correct and add to reference genes generated with intermediate and short reads. *GigaScience* **6**, 1–16 (2017).
47. Wingett, S. et al. HiCUP: pipeline for mapping and processing Hi-C data. *F1000Res* **4**, 1310 (2015).

48. Rhie, A. et al. Towards complete and error-free genome assemblies of all vertebrate species. *Nature* **592**, 737–746 (2021).
49. Zhang, X., Zhang, S., Zhao, Q., Ming, R. & Tang, H. Assembly of allele-aware, chromosomal-scale autopolyploid genomes based on Hi-C data. *Nat. Plants* **5**, 833–845 (2019).
50. Durand, N. C. et al. Juicebox provides a visualization system for Hi-C contact maps with unlimited zoom. *Cell Syst.* **3**, 99–101 (2016).
51. Li, H. & Durbin, R. Fast and accurate short read alignment with Burrows-Wheeler transform. *Bioinformatics* **25**, 1754–1760 (2009).
52. Simao, F. A., Waterhouse, R. M., Ioannidis, P., Kriventseva, E. V. & Zdobnov, E. M. BUSCO: assessing genome assembly and annotation completeness with single-copy orthologs. *Bioinformatics* **31**, 3210–3212 (2015).
53. Hubley, R. & Smit, A. RepeatModeler, version 1.0.11. *GitHub*. https://github.com/Dfam-consortium/RepeatModeler (2018).
54. Xu, Z. & Wang, H. LTR_FINDER: an efficient tool for the prediction of full-length LTR retrotransposons. *Nucleic Acids Res.* **35**, W265–W268 (2007).
55. Ou, S. & Jiang, N. LTR_retriever: a highly accurate and sensitive program for identification of long terminal repeat retrotransposons. *Plant Physiol.* **176**, 1410–1422 (2018).
56. Tarailo-Graovac, M. & Chen, N. Using RepeatMasker to identify repetitive elements in genomic sequences. *Curr. Protoc. Bioinform.* **25**, 4.10.1–4.10.14 (2009).
57. Chan, P. P., Lin, B. Y., Mak, A. J. & Lowe, T. M. tRNAscan-SE 2.0: improved detection and functional classification of transfer RNA genes. *Nucleic Acids Res.* **49**, 9077–9096 (2021).
58. Nawrocki, E. P. & Eddy, S. R. Infernal 1.1: 100-fold faster RNA homology searches. *Bioinformatics* **29**, 2933–2935 (2013).
59. Stanke, M., Diekhans, M., Baertsch, R. & Haussler, D. Using native and syntenically mapped cDNA alignments to improve de novo gene finding. *Bioinformatics* **24**, 637–644 (2008).
60. Delcher, A. L., Bratke, K. A., Powers, E. C. & Salzberg, S. L. Identifying bacterial genes and endosymbiont DNA with Glimmer. *Bioinformatics* **23**, 673–679 (2007).
61. Camacho, C. et al. BLAST plus: architecture and applications. *BMC Bioinforma.* **10**, 421 (2009).
62. Slater, G. S. & Birney, E. Automated generation of heuristics for biological sequence comparison. *BMC Bioinforma.* **6**, 31 (2005).
63. Holt, C. & Yandell, M. MAKER2: an annotation pipeline and genome-database management tool for second-generation genome projects. *BMC Bioinforma.* **12**, 491 (2011).
64. Emms, D. M. & Kelly, S. OrthoFinder: phylogenetic orthology inference for comparative genomics. *Genome Biol.* **20**, 238 (2019).
65. Yang, X. et al. The *Kalanchoë* genome provides insights into convergent evolution and building blocks of crassulacean acid metabolism. *Nat. Commun.* **8**, 1899 (2017).
66. Wai, C. et al. Time of day and network reprogramming during drought induced CAM photosynthesis in *Sedum album*. *PLoS Genet.* **15**, e1008209 (2019).
67. Fu, Y. et al. Draft genome sequence of the Tibetan medicinal herb *Rhodiola crenulata*. *GigaScience* **6**, gix033 (2017).
68. Xu, W. et al. Genome sequences and population genomics reveal climatic adaptation and genomic divergence between two closely related sweetgum species. *Plant J.* **118**, 1372–1387 (2024).
69. Liu, L. et al. Phylogenomic and syntenic data demonstrate complex evolutionary processes in early radiation of the rosids. *Mol. Ecol. Resour.* **23**, 1673–1688 (2023).
70. Lamesch, P. et al. The *Arabidopsis* information resource (TAIR): improved gene annotation and new tools. *Nucleic Acids Res.* **40**, D1202–D1210 (2012).
71. Pei, T. et al. The genome of *Tripterygium wilfordii* and characterization of the celastrol biosynthesis pathway. *GigaByte* **2021**, gigabyte14 (2021).
72. Huang, S. et al. The genome of the cucumber, *Cucumis sativus* L. *Nat. Genet.* **41**, 1275–1281 (2009).
73. Vega, D. et al. Red clover (*Trifolium pratense* L.) draft genome provides a platform for trait improvement. *Sci. Rep.* **5**, 17394 (2015).
74. Kang, Y. et al. Genome sequence of mungbean and insights into evolution within *Vigna* species. *Nat. Commun.* **5**, 5443 (2014).
75. Annarita, M. et al. High-quality chromosome-scale assembly of the walnut (*Juglans regia L.*) reference genome. *GigaScience* **9**, giaa050 (2020).
76. Jia, H. et al. The red bayberry genome and genetic basis of sex determination. *Plant Biotechnol. J.* **17**, 397–409 (2019).
77. Wang, Z. et al. The genome of flax (*Linum usitatissimum*) assembled de novo from short shotgun sequence reads. *Plant J.* **72**, 461–473 (2012).
78. Tuskan, G. A. et al. The genome of black cottonwood, *Populus trichocarpa* (Torr. & Gray). *Science* **313**, 1596–1604 (2006).
79. Healey, A. L. et al. Pests, diseases, and aridity have shaped the genome of *Corymbia citriodora*. *Commun. Biol.* **4**, 537 (2021).
80. Wang, X. et al. Genomic analyses of primitive, wild and cultivated citrus provide insights into asexual reproduction. *Nat. Genet.* **49**, 765–772 (2017).
81. He, N. et al. Draft genome sequence of the mulberry tree *Morus notabilis*. *Nat. Commun.* **4**, 2445 (2013).
82. Kenta, S. et al. The genome sequence of sweet cherry (*Prunus avium*) for use in genomics-assisted breeding. *DNA Res.* **24**, 499–508 (2017).
83. Verde, I. et al. The high-quality draft genome of peach (*Prunus persica*) identifies unique patterns of genetic diversity, domestication and genome evolution. *Nat. Genet.* **45**, 487–494 (2013).
84. Shi, X. et al. The complete reference genome for grapevine (*Vitis vinifera* L.) genetics and breeding. *Hortic. Res.* **10**, uhad061 (2023).
85. Gergo, P. et al. Genomes of the Venus flytrap and close relatives unveil the roots of plant carnivory. *Curr. Biol.* **30**, 2312–2320 (2020).
86. Procko, C., Chory, J. & Pirro, S. The genome sequences of 17 species of carnivorous plants. *Biodivers. Genomes* **2023**, 001c.90164 (2023).
87. Saul, F. et al. Subgenome dominance shapes novel gene evolution in the decaploid pitcher plant *Nepenthes gracilis*. *Nat. Plants* **9**, 2000–2015 (2023).
88. Hartmann, S. et al. Annotated genome sequences of the carnivorous plant *Roridula gorgonias* and a non-carnivorous relative, *Clethra arborea*. *BMC Res. Notes* **13**, 426 (2020).
89. Clouse, J. W. et al. The amaranth genome: genome, transcriptome, and physical map assembly. *Plant Genome* **9**, 107 (2016).
90. Collins, K. et al. SpinachBase: a central portal for spinach genomics. *Database* **2019**, baz072 (2019).
91. Hufford, M. B. et al. De novo assembly, annotation, and comparative analysis of 26 diverse maize genomes. *Science* **373**, 655–662 (2021).
92. Zhang, L. et al. The water lily genome and the early evolution of flowering plants. *Nature* **577**, 79–84 (2020).
93. Zwaenepoel, A. & Van de Peer, Y. wgd-simple command line tools for the analysis of ancient whole-genome duplications. *Bioinformatics* **35**, 2153–2155 (2019).
94. Katoh, K. & Standley, D. M. MAFFT multiple sequence alignment software version 7: improvements in performance and usability. *Mol. Biol. Evol.* **30**, 772–780 (2013).
95. Rice, P., Longden, I. & Bleasby, A. EMBOSS: the European molecular biology open software suite. *Trends Genet* **16**, 276–277 (2000).
96. Yu, G. et al. clusterProfiler: an R package for comparing biological themes among gene clusters. *OMICS* **16**, 284–287 (2012).

97. Kowalczyk, A. et al. RERconverge: an R package for associating evolutionary rates with convergent traits. *Bioinformatics* **35**, 4815–4817 (2019).
98. Löytynoja, A. Phylogeny-aware alignment with PRANK. *Methods Mol. Biol.* **1079**, 155–170 (2014).
99. Kosakovsky, P. et al. HyPhy 2.5—a customizable platform for evolutionary hypothesis testing using phylogenies. *Mol. Biol. Evol.* **37**, 295–299 (2020).
100. Zhang, X.-J. GC–MS raw data for: Ecological and genomic evidence for carnivory in Saxifraga. *Zenodo*. https://doi.org/10.5281/zenodo.19695105 (2026).
101. Zhang, X.-J., & Fu, Q.-S. R scripts for: Carnivory discovered in the flowering plant *Saxifraga* confirming Darwin's prediction. *Zenodo*. https://doi.org/10.5281/zenodo.20322891 (2026).
102. Lin, N. Genome-based converge analysis. *Zenodo*. https://doi.org/10.5281/zenodo.20411937 (2026).
103. De Bie, T., Cristianini, N., Demuth, J. P. & Hahn, M. W. CAFE: a computational tool for the study of gene family evolution. *Bioinformatics* **22**, 1269–1271 (2006).

Acknowledgements

We thank Drs. Fei Li and Wei Chang (Service Center for Experimental Biotechnology, Kunming Institute of Botany, CAS) for assistance with isotopic and GC–MS analyses; Rong Ma and Shuang Cun (Kunming Institute of Botany, CAS) for *Drosophila* culture and isotopic labeling; and Drs. Shuiqing Liang and Ting Tang (Institutional Center for Shared Technologies and Facilities, Xishuangbanna Tropical Botanical Garden, CAS) for assistance with isotopic analyses. We also appreciate Dr. Zhijia Gu (Platform for Multi-dimensional Imaging and Diversity Analysis, Kunming Institute of Botany, CAS) for support with fluorescence imaging. We are grateful to Dr. Lishen Qian (Kunming Botanical Garden, Kunming Institute of Botany, CAS) and Drs. Lili Shao and Kuiyan Zhang (Institute of Zoology, CAS) for their invaluable help in insect prey identification. We thank Dr. Wenguang Sun (Yunnan Normal University) for chromosome karyotype analyses. We also acknowledge the Kunming Botanical Garden (Kunming Institute of Botany, CAS), particularly Shen Wang, Kangzheng Jiang, and Hanrun Li, for greenhouse facilities and plant cultivation support.

Author contributions

H.S. conceived the project. H.S., D.E.S., T.D., and B.S. designed the project. X.J.Z., E.N.X., T.D., H.C.W., B.S., and X.H.H. carried out field investigations and sample collections. X.J.Z., X.H.H., P.R.L., J.T.C., and Q.S.F. conducted the enzymatic experiments. X.J.Z., B.S., and T.D. performed the isotope labeling experiments. N.L. and T.D. conducted the genome data analyses. X.J.Z., N.L., T.D., H.C.W., B.S., H.S., and D.E.S. wrote the original paper. All authors revised the paper.

Funding

This work was supported by grants from the Second Tibetan Plateau Scientific Expedition and Research (STEP) program (2024QZKK0200 to H.S., 2019QZKK0502 to H.S.), the National Natural Science Foundation of China (32322006 to T.D.), the Joint Fund of the National Natural Science Foundation of China (U23A20149 to H.S.), the National Key R&D Program of China (2024YFF1306700 to T.D.), the Yunnan Key R&D Program (202403AC00028 to H.S.), and the Yunnan Academician Free Exploration Project (to H.S.).

Competing interests

The authors declare no competing interests.

Additional information

Supplementary information The online version contains supplementary material available at https://doi.org/10.1038/s41467-026-75288-y.

Correspondence and requests for materials should be addressed to Tao Deng, Douglas E. Soltis or Hang Sun.

Peer review information *Nature Communications* thanks Toshihiro Murata and the other anonymous reviewers for their contribution to the peer review of this work. A peer review file is available.